INTERNATIONAL JOURNAL FOR NUMERICAL METHODS IN FLUIDS
Int. J. Numer. Meth. Fluids 2006; **50**:263–273
Published online 21 September 2005 in Wiley InterScience (www.interscience.wiley.com). DOI: 10.1002/fld.1046

Microstructure development in concentrated suspensions in a spinning ball rheometer[§]

Anne M. Grillet[*,†] and Lisa A. Mondy[‡]

Sandia National Laboratories, Albuquerque, NM 87185-0834, U.S.A.

SUMMARY

The spinning ball rheometer has been proposed as a method to measure the microstructure effect on the bulk rheological properties of concentrated suspensions. Recent experiments have shown that the measured extra torque on the spinning ball decreases as the radius of the spinning ball becomes comparable to the size of the suspended particle. We have performed a series of three-dimensional boundary element calculations of the rheometer geometry to probe the microstructure effects that contribute to that apparent *slip*. We present a series of quasi-static results based on random initial configurations as well as fully three-dimensional transient calculations, both of which are compared to the available experimental data. For the two cases, the apparent viscosity decreased as the size of the spinning ball decreased relative to the suspended particle. Comparison of the quasi-static and transient simulations indicates that the microstructure development is critical even at short times. In the transient calculations, the viscosity was observed to increase substantially relative to the torque based on the random initial configuration. Published in 2005 by John Wiley & Sons, Ltd.

KEY WORDS: suspension; microstructure; boundary element method; flow-induced structure; rheology

1. INTRODUCTION

Mixtures of solid particles suspended in a viscous liquid are ubiquitous in applications ranging from polymer processing, dyes, printing and coatings. In many cases, the product quality depends on the distribution of the suspended particles as they can affect many rheological and material properties. Unfortunately, the complex processing flows can frequently cause non-uniform particle concentrations [1–4]. Whereas there exists a significant body of work regarding the continuum rheology of suspensions in shear flows, i.e. References [2, 5–8] among

*Correspondence to: Anne M. Grillet, Sandia National Laboratories, Albuquerque, NM 87185-0834, U.S.A.
†E-mail: amgrill@sandia.gov
‡E-mail: lamondy@sandia.gov

Contract/grant sponsor: U.S. Department of Energy; contract/grant number: DE-AC04-94AL85000

Received 9 December 2004
Revised 8 June 2005
Accepted 10 June 2005

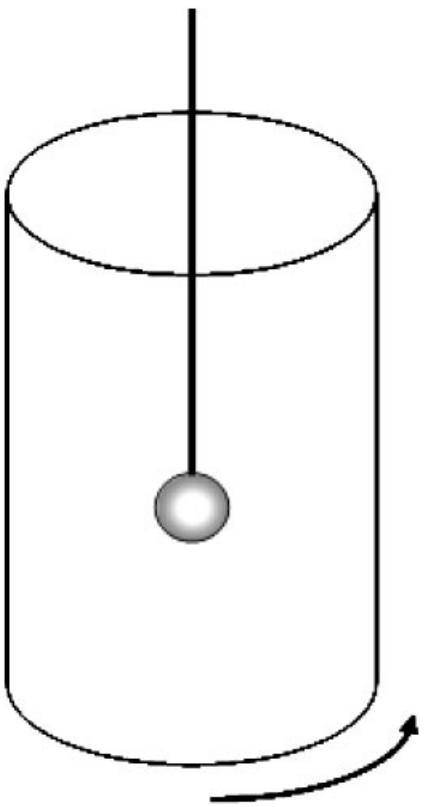

Figure 1. Schematic of the spinning ball rheometer. The suspended ball is rotated relative to the suspension and the resulting torque is used to measure the apparent viscosity of the suspension.

many others, the non-local effects which occur when the suspended particle size is on the same length scale as the flow are not well understood. There is currently a dearth of experimental and numerical tools to probe the non-local rheology of suspensions or to understand their behaviour in complex mixed extensional flows.

The spinning ball rheometer has been proposed as a method to explore complex rheological phenomena in concentrated suspensions such as the apparent *slip* at small length scales. A schematic of the spinning ball rheometer is shown in Figure 1. The suspended ball is rotated relative to the suspension and the resulting torque is used to measure the apparent viscosity of the suspension. Experimental measurements have shown that the measured extra torque (relative to the torque measured in the fluid without particles) depends on the ratio of the radius of the spinning ball r_b to the size of the suspended particle r_p [9]. For relatively large spinning balls, the measured viscosity is comparable to other experimental methods for determining the (bulk) suspension viscosity, but as the spinning ball decreases in size, the measured viscosity drops substantially [9, 10]. This apparent *slip* is due to the different length scales in the suspension that are probed by the different sizes of spinning balls. As the size of the spinning ball decreases, the length scale probed decreases as well until in the limit of

infinitely small spinning ball, the viscosity of the suspending fluid is measured [10]. Thus, the spinning ball rheometer provides a valuable tool to probe the full range of length scales present in these complex multiphase mixtures.

In addition to probing different length scales, the spinning ball device also exhibits a range of interesting dynamic phenomena. When starting from an initially well-mixed state, the measured torque is seen to increase over the first several revolutions of the spinning ball. These initial transients were not measurement artifacts as they were not present in calibration experiments on Newtonian liquids and they were observed for suspensions both experimentally and numerically. For large strains, the observed torque slowly decreased over a period of several hundred ball revolutions to a final steady-state value. Experimental results suggest that the decrease is due to shear-induced migration of the particles away from the high-shear regions near the spinning ball. The cause of the initial increase in the measured viscosity is not well understood, though it is believed to be caused by changes in the suspension microstructure due to the onset of flow [9].

In order to probe the microstructural causes of the transients observed during the onset of flow in suspensions, we employ transient three-dimensional boundary element simulations. Boundary element methods provide a significant advantage over finite element or finite difference methods because only the surfaces of the domain are discretized. Finite element and difference methods generally require a grid for the entire volume. Lagrangian or arbitrary Lagrangian–Eulerian formulations generally only mesh the fluid phase. While this is topologically challenging for a stationary simulation, transient mapping of the fluid phase requires frequent remeshing, limiting these techniques to dilute suspensions [11, 12]. More recently, Eulerian methods have been implemented which track the moving particles as they pass through a stationary mesh. These suffer from difficulties when the distances between particles decreases to less than the element size and have thus far only been implemented for dilute or two-dimensional simulations [13, 14].

The direct boundary element method was first employed by Youngren and Acrivos to study Stokes flow around single particles [15] and has since been employed by others to study the dynamics of multiple particles [16–19]. Previous works have shown that boundary element simulations can qualitatively capture the complex dynamic physics observed experimentally in many suspension flows [5, 20–22]. Our previous work investigating the spinning ball rheometer has validated that boundary element simulations can capture the apparent slip observed in the measured viscosity in this geometry [9]. Here, we will further analyse the short time dynamics in this geometry to understand how changes in the suspension microstructure give rise to the changes in the short time increase in the apparent viscosity observed experimentally. Section 2 describes the boundary element method used with the analysis of the microstructure presented in Section 3.

2. METHOD

Fully three-dimensional boundary element calculations were performed for a relatively concentrated suspension using a range of suspended particle to spinning ball size ratios r_p/r_b. The direct boundary element simulation method used for these calculations has been described in detail elsewhere [22–24], but a brief description is presented here for completeness. The incompressible low-Reynold's-number flow of the interstitial fluid between the particles is

governed by the standard continuity and Stokes flow equations:

$$\nabla \cdot u = 0; \quad \mu \nabla^2 u = \nabla p$$

where u is the velocity in the fluid phase, p is the pressure and μ is the viscosity of the suspending fluid. It can be shown that the governing velocity boundary integral equation is given by

$$c_{ij}(x)u_j(x) + \int_\Gamma q^*_{ijk}(x,y)n_j(y)u_k(y)\,\mathrm{d}\Gamma(y) = -\int_\Gamma u^*_{ij}(x,y)f_j(y)\,\mathrm{d}\Gamma(y)$$

where u^*_{ij} and q^*_{ijk} are the fundamental singular Stokes velocity and stress fields, respectively.

$$u^*_{ij}(x,y) = \frac{1}{8\pi\mu r}\left(\delta_{ij} + x_{,i}\, x_{,j}\right)$$

$$q^*_{ijk} = -\frac{3r_{,i}\, r_{,j}\, r_{,k}}{4\pi r^2}; \quad r = |x - y|$$

Additionally, c_{ij} is a coefficient tensor, f_j are the traction vectors and n_j are the normal vectors along the boundary $\Gamma(y)$. Commas indicate differentiation with respect to the appropriate Cartesian coordinate.

For the spinning ball rheometer geometry, the velocities are specified along the cylinder and spinning ball boundaries. However, on the surfaces of the suspended particles, the velocities and tractions are not known *a priori*. In order to close the system of equations, several constraints are applied. A kinematic condition is enforced so that each suspended particle behaves as a rigid solid with a no-slip boundary condition at the surface.

$$u_i = u_i^p + \varepsilon_{ijk}\Omega_j^p x_k$$

where u_i^p and Ω_i^p are the linear and angular particle velocity vectors for the pth particle and x_j is the displacement vector of a point on the surface of a suspended sphere relative to its centre. Consistent with the Stokes approximation, particle accelerations are neglected and the neutrally buoyant suspended particles are assumed to be force and torque free.

$$\int_{\Gamma_p} f_i\,\mathrm{d}\Gamma = 0; \quad \int_{\Gamma_p} \varepsilon_{ijk}\, x_j^p f_k\,\mathrm{d}\Gamma = 0$$

The boundary element chosen for this calculation is a superparametric element in which the boundary geometry is quadratically approximated. An adaptive quadrature technique is used where the number of Gauss points within an element is a function of an integration severity number [24].

For the rheometer simulations, the spinning ball was placed in the centre of a cylinder of dimensionless height of 10 and diameter of 10 which was filled with fluid of dimensionless viscosity $\mu_N = 1$. For each simulation, 220 spherical particles were placed in the viscometer domain using randomly generated positions. The sizes of both the particles and spinning ball were chosen to achieve a given size ratio and particle volume fraction c. For each case the domain was meshed with 122 nodes per particle and 5762 on the surrounding cylinder as

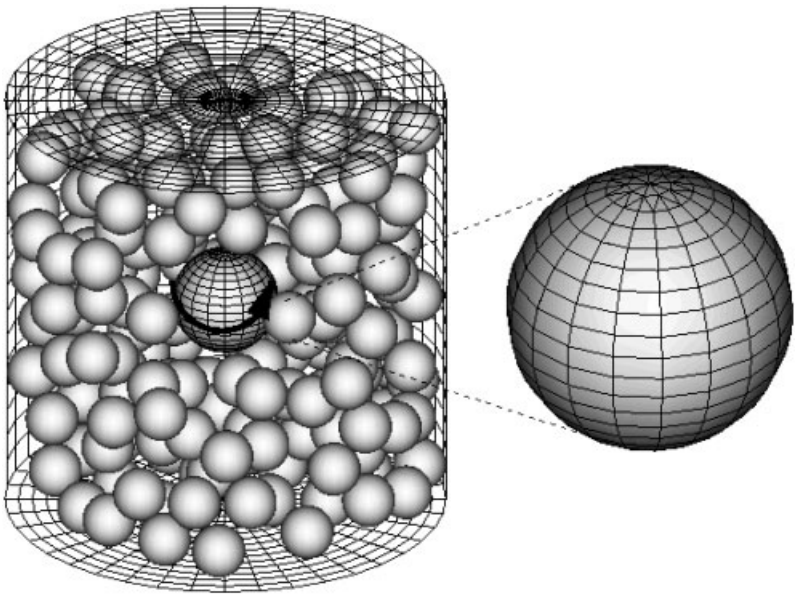

Figure 2. Representative mesh used for spinning ball calculations for the case $r_p/r_b = 0.25$. Suspended particles in front of the spinning ball have been made transparent.

shown in Figure 2. The spinning ball was meshed with 362 nodes for most of the simulations except for calculations with the largest spinning ball $r_p/r_b = 0.25$ where 1522 nodes were used. The most important limiting factor for these simulations is the finite size of the container (specifically the radius) that is in turn limited by the number of particles that can be simulated. Figure 3 shows error in the calculated Newtonian torque for various cylinder sizes and mesh resolutions on the cylinder walls and spinning ball relative to Kirchoff's theory for the torque on a spinning ball in an infinite pool. As the size of the spinning ball increases relative to the cylinder radius, the error caused by the increased drag due to the presence of the sidewalls increases rapidly. Thus, for $r_p/r_b = 0.25$ which corresponds to the largest ball size shown in Figure 3, end wall effects are increasing the apparent Newtonian viscosity by 10%. To compensate for these finite size effects, all of the suspension viscosity results will be presented scaled by the calculated Newtonian viscosity. Increasing the cylinder height or the mesh resolution on the cylinder or the spinning balls had a much more modest impact on the measured error than changes in the cylinder radius. We also investigated the effect of increasing the mesh refinement on both the particles and the spinning ball for calculations with suspended particles. Since the torque is measured on the spinning ball, we found that the simulation results were more sensitive to the refinement on the spinning ball than increases in particle mesh refinement. Doubling the number of elements on the particles for $r_p/r_b = 0.5$ changed the measured torque by less than 0.5%, while halving the number of elements on the spinning ball changed the torque by 3%. Thus, the spinning ball has a relatively higher mesh density than the particles.

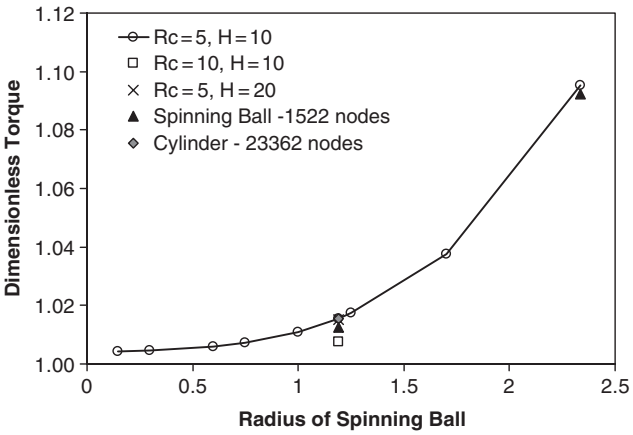

Figure 3. Comparison of measured Newtonian viscosity as a function of the radius of the ball for various cylinder geometries and mesh resolutions.

As in all numerical simulations, compromises are required to achieve the maximum fidelity to the true physics within the limitations of available computational resources. All of these calculations were performed on ASCI Red, the world's first TeraOPS supercomputer when it was brought on line in 1997. This supercomputer resides at Sandia National Laboratories and consists of 4500 nodes containing two upgraded 300 MHz Pentium II processors which share 128 MB of memory. With 256 processors, a simulation consisting of 220 suspended particles with the standard mesh refinement detailed above for the largest spinning ball progressed half of a strain unit (one revolution of the spinning ball) in 24 hours of computational time. We determined this system size, specifically the number of suspended particles, to be the largest that was practical considering the required ensemble sizes and the various size ratios which were of interest. We also limited our investigation to a single volume fraction of 25%. Larger volume fraction calculations were prohibitively expensive, and experimental results determined that this volume fraction showed the same dynamic behaviour as more concentrated suspensions up to volume fractions of 45% [9]. This was also the lowest volume fraction for which experimental data were available for comparison.

For each size ratio, an initial Newtonian torque L_N was calculated by performing a simulation without particles in the geometry. To calculate the suspension viscosity, two methods were used. For all cases, an instantaneous torque was calculated using the random initial particle configuration. This was initially believed to be an accurate method to compare to the short time experimental results since the suspensions were stirred before each experiment to achieve a uniform particle distribution. Because the torque was observed to be highly dependent on the arrangement of the suspended particles, all results were ensemble averaged over many initial configurations in the same manner as the experimental results were averaged over several experiments. Dynamic torque measurements can also be determined by performing transient simulations starting from the random initial configurations. Since these systems are not ergodic, results from the transient simulations were also ensemble averaged. The calculated values of the torque are presented in terms of the reduced viscosity ($\mu_r = \mu_s/\mu_N$) which equals the ratio of the suspension torque to L_N.

3. RESULTS

For a fairly concentrated suspension ($c = 0.25$), suspension viscosities calculated from ensemble averages of 10 random initial configurations ('quasi-static') are compared to experimentally measured relative suspension viscosities in Figure 4. The experimental data presented in the figure were initial viscosities that were averaged over the first four ball revolutions. The boundary element simulations are seen to underpredict the expected viscosity of the suspension as has also been noted in previous 'quasi-static' calculations on dilute systems [9]. This graph clearly illustrates the apparent *slip* phenomena—as the size of the spinning ball decreases, the measured viscosity decreases approaching the suspending fluid viscosity.

To test the possible influence of the use of a random particle configuration on the torque measurements, transient calculations were performed for several ratios of the spinning ball to particle sizes. In other flows of concentrated suspensions, flow-induced structure formation has been observed [25]. By performing dynamic calculations, the possible effects of flow-induced structure can be included in the comparison to the experimental results. For each of the 10 initial configurations, the flow is simulated for 5–10 revolutions of the spinning ball and the transient torques are ensemble averaged. Figure 5 shows the combined transient torque data for 10 configurations for the four size ratios investigated, as well as the resulting averaged torque. For cases where the spinning ball is larger than the suspended particles, the torque is seen to increase when the flow is started, whereas for $r_p/r_b > 1$, the change in the torque is small ($< 0.5\%$ for $r_p/r_b = 2$). After several revolutions, the averaged torque stops increasing and approximately levels out. The value is then averaged in time and used to calculate the dynamic relative viscosity shown in Figure 4. This plateau region is by no means a steady-state viscosity, but rather is thought to be a more accurate comparison to the averaged initial torque measured in the experiments [9].

The shear thickening behaviour observed in the dynamic simulations are clearly caused by changes to the microstructure due to the onset of flow. This effect appears to be separate from

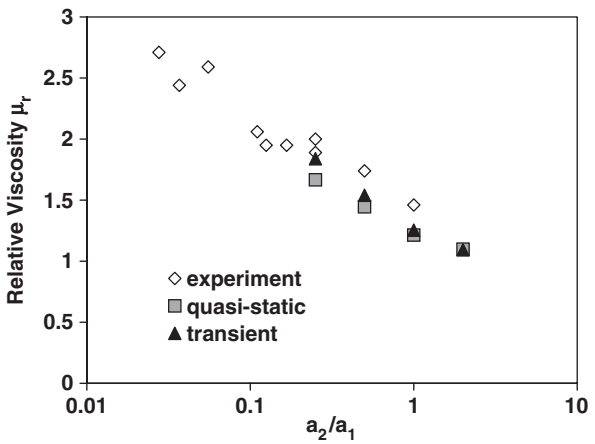

Figure 4. Comparison of the relative viscosity from both experimental measurements [9] and boundary element simulations at $c = 0.25$ as a function of particle size ratio.

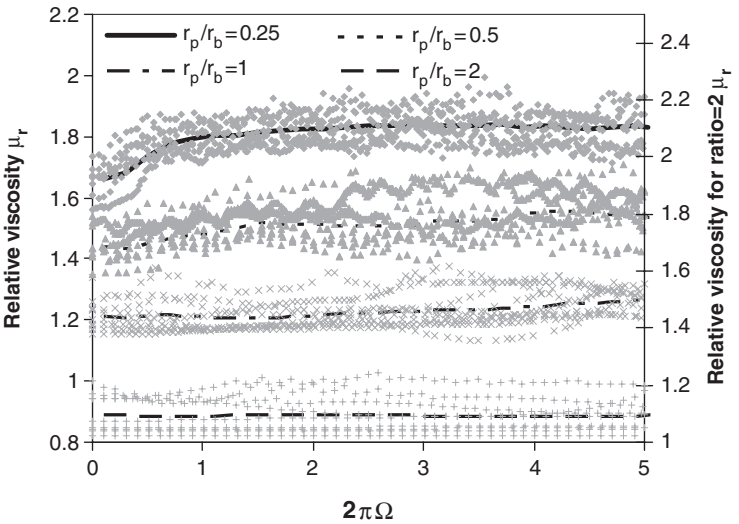

Figure 5. Ensemble averaged torque (lines) compared to transient torque for 10 different initial configurations (symbols). To prevent overlap of the data, for a size ratio of 2, the data are plotted on the right hand axis.

the particle migration that occurs at large strains [2], as the calculated torque reaches a quasi-steady state after just a few revolutions of the spinning ball. A short time initial increase in viscosity was also observed by Leighton and Acrivos in their experiments on Couette flows of suspensions. However, when the inner cylinder of the Couette device was lowered into the suspension, the resulting flow in the channel resulted in significant variations in particle concentration inside the experimental apparatus as originally observed by Karnis and Mason [26]. Thus, at the start-up of flow in their experiment, the increase in the observed viscosity was due to concentration gradient induced particle migration. Since our initial particle configuration is randomly generated, similar effects are not expected in these results. Whereas thixotropic behaviour is generally attributed to the destruction of an equilibrium structure that results in a decrease of the measured viscosity, an increase in viscosity can be attributed to a build-up of structure at the onset of flow [27]. To determine if the increase in viscosity was due to the formation of a particle microstructure, we have tracked particle aggregation during the transient simulations. In this work, a *cluster* was defined as a group of neighbouring particles where the inter-particle distance between two neighbours was less than 5% of the particle radius. With the starting random initial configuration, very few particles had neighbours, so each simulation began with almost 200 *clusters*, most containing only one particle (Figure 6). As the spinning ball rotates and particles advecting at non-uniform velocities are moved closer to each other, pairs of particles and eventually much larger clusters began to form as shown in Figure 6.

As shown in Figure 7(a), the degree of flow-induced structure correlates closely to the changes in the viscosity for the dynamic simulations relative to the quasi-static simulation results. The larger spinning balls generate more aggregate formation than the smaller spinning balls. For the smallest spinning ball, there is almost no change from the initial configuration

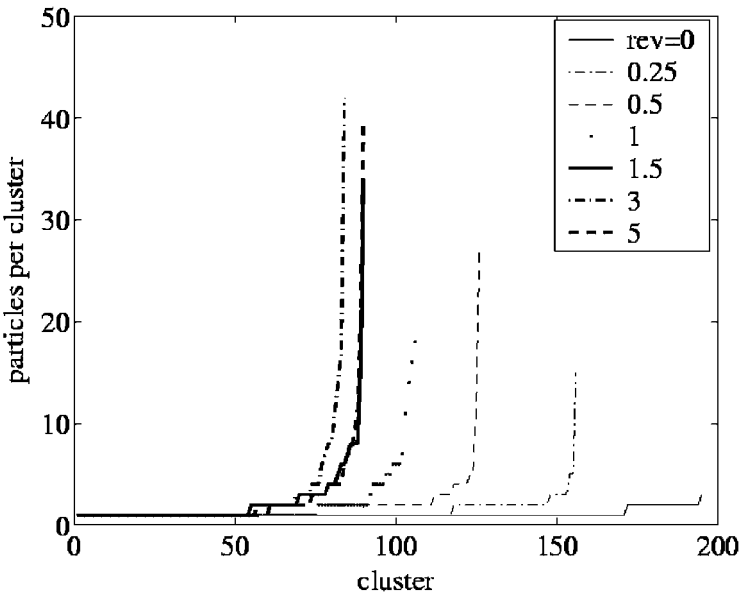

Figure 6. Number of particles in each *cluster* for size ration $r_p/r_b = 0.25$ for several strains.

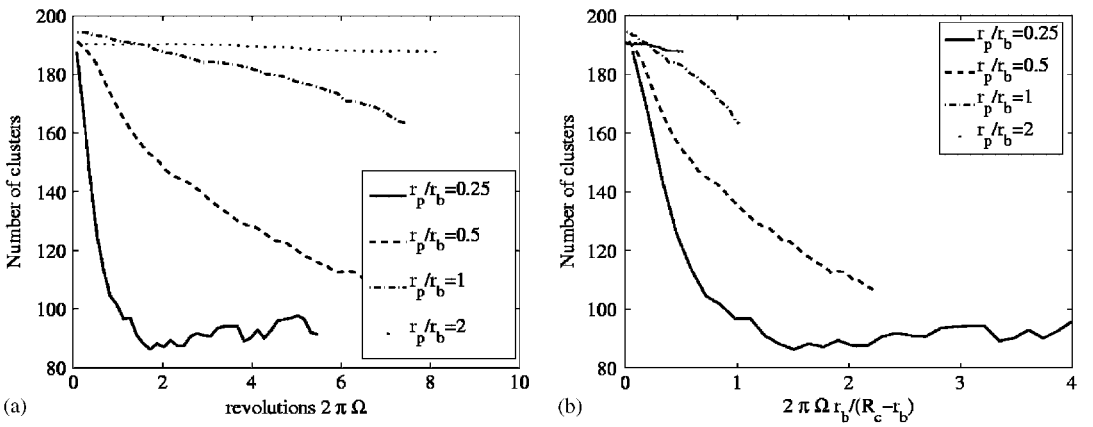

Figure 7. Number of clusters as a function of two strain measures: (a) the revolutions of the spinning ball; and (b) strain scaled with shear rate between spinning ball and cylinder wall.

with most particles never having a neighbour. Due to the complex three-dimensional nature of the flow, there are many possible strain measures available. Up to this point we have presented transient results as a function of spinning ball revolutions ($2\pi\Omega$) which is the correct strain measure for collapsing shear-induced migration effects [2, 9]. Unfortunately, this strain measure does not collapse the cluster development curves for various spinning ball size ratios. We have tried several alternate strain measures including the one shown in Figure 7(b)

that is defined using the shear rate between the spinning ball and the cylinder wall. None of these strain measures was able to remove the size dependence of the development of the flow-induced structure, possibly indicating that it is related to the apparent *slip* phenomena.

4. DISCUSSION

The boundary element simulations confirm the apparent *slip* as a function of the size ratio between the spinning ball and suspended particle that was observed experimentally. Furthermore, the particle configuration information available in the simulations provides detailed insights into the microstructural causes of the *slip* behaviour and also the rapid increase in the viscosity after onset of flow. Small spinning balls probe small length scales in the suspension and for large particle size ratios r_p/r_b tend to measure the properties of the suspending fluid. In these cases, the flow does not induce anti-thixotropic behaviour related to the development of flow-induced structure. Larger spinning balls cause large deformations in the particle microstructure and probe the large cluster formation and dynamics in the suspension. At these larger length scales, the development of flow-induced structure and anti-thixotropic behaviour can be observed. By manipulating the size scales, the spinning ball rheometer provides a unique tool to examine the multiple length scales present in the suspension microstructure and the dynamic formation of flow-induced structure at the various length scales.

These simulations for a spinning ball rheometer also shed light on more general dynamics observed in suspension flows. When the flow is first started, there is an initial increase in the measured viscosity of the suspension. Whereas this phenomenon has been observed previously in experiments, it was generally attributed to start-up effects. We found that the initial increase was actually caused by a rapid initial rearrangement of the particle microstructure from the initial random configuration. This has important implications for the modelling of suspension flows. Taking a quasi-static approach using a random initial configuration of particles, though significantly simpler than performing transient simulations, did not accurately predict the initial viscosity of the suspension. This disparity was most apparent for our largest spinning ball and would be expected to be more important as even longer length scales were probed such as in a bulk viscosity measurement.

ACKNOWLEDGEMENTS

Sandia is a multiprogram laboratory operated by Sandia Corporation, a Lockheed Martin Company for the United States Department of Energy's National Nuclear Security Administration under contract DE-AC04-94AL85000. The authors would like to acknowledge support for this work by the U.S. Department of Energy, Division of Engineering and Geosciences, Office of Basic Energy Sciences.

REFERENCES

1. Eckstein EC, Bailey DG, Shapiro AH. Self-diffusion of particles in shear flow of a suspension. *Journal of Fluid Mechanics* 1997; **79**:191–208.
2. Leighton DT, Acrivos A. The shear induced migration of particles in concentrated suspensions. *Journal of Fluid Mechanics* 1987; **181**:415–439.
3. Altobelli SA, Fukushima E, Mondy LA. Nuclear magnetic resonance imaging of particle migration in suspensions undergoing extrusion. *Journal of Rheology* 1997; **41**:1105–1115.
4. Tetlow NA, Graham AL, Ingber MS, Subia SR, Mondy LA, Altobelli SA. Particle migration in a Couette apparatus: experiment and modeling. *Journal of Rheology* 1999; **42**:307–327.

5. Gadala-Maria F, Acrivos A. Shear-induced structure in a concentrated suspension of solid spheres. *Journal of Rheology* 1980; **24**:799–811.
6. Phillips RJ, Armstrong RC, Brown RA, Graham AL, Abbott JR. A constitutive equation for concentrated suspensions that accounts for shear-induced particle migration. *Physics of Fluids A* 1992; **4**:30–40.
7. Brady JF, Morris JF. Microstructure of strongly sheared suspensions and its impact on rheology and diffusion. *Journal of Fluid Mechanics* 1997; **348**:103–139.
8. Zarraga IE, Leighton DT. Measurement of an unexpectedly large shear-induced self-diffusivity in a dilute suspension of spheres. *Physics of Fluids* 2002; **14**(7):2194–2201.
9. Mondy LA, Grillet AM, Pacheco G, Henfling J, Ingber MS, Graham AL, Brenner H. Apparent slip at the surface of a ball spinning in a concentrated suspension. *Journal of Fluid Mechanics*, in press.
10. Almog Y, Brenner H. Non-continuum anomalies in the apparent viscosity experienced by a test sphere moving through an otherwise quiescent suspension. *Physics of Fluids* 1997; **9**:16–22.
11. Hu HH, Patankar NA, Zhu MY. Direct numerical simulation of fluid–solid systems using arbitrary Lagrangian–Eulerian technique. *Journal of Computational Physics* 2001; **169**:427–462.
12. Jaeger M, Carin M. The front tracking ALE method: application to a model of the freezing of cell suspensions. *Journal of Computational Physics* 2002; **179**:704–735.
13. Hwang WR, Hulsen MA, Meijer HEH. Direct simulation on particle suspensions in sliding bi-periodic frames. *Journal of Computational Physics* 2004; **194**:742–772.
14. Wagne GJ, Ghosal S, Liu WK. Particulate flow simulations using lubrication theory solution enrichment. *International Journal for Numerical Methods in Engineering* 2003; **56**:1261–1289.
15. Youngren GK, Acrovis A. Stokes flow past a particle of arbitratry shape: a numerical method of solution. *Journal of Fluid Mechanics* 1979; **69**(2):377–402.
16. Tran-Cong T, Phan-Thien N, Graham AL. Stokes problems of multiparticle systems: periodic arrays. *Physics of Fluids A* 1991; **2**(5):666–673.
17. Vincent J, Phan-Thien N, Tran-Cong T. Sedimentation of multiple particles of arbitrary shape. *Journal of Rheology* 1991; **35**(1):1–26.
18. Karilla SJ, Fuentes YO, Kim S. Parallel computational strategies for hydrodynamic interactions between rigid particles of arbitrary shape in a viscous fluid. *Journal of Rheology* 1989; **33**(6):913–947.
19. Pozrikidis C. Dynamical simulation of the flow of suspensions: wall bounded and pressure driven channel flow. *Industrial and Engineering Chemistry Research* 2002; **41**:6312–6322.
20. Brady JR, Bossis G. The rheology of concentrated suspensions of spheres in simple shear flow by numerical simulation. *Journal of Fluid Mechanics* 1985; **155**:105–129.
21. Brady JR, Bossis G. Stokesian dynamics. *Annual Review of Fluid Mechanics* 1998; **20**:111–157.
22. Dingman SE, Ingber MS, Mondy LA, Abbott JR, Brenner H. Particle tracking in three-dimensional Stokes flow. *Journal of Rheology* 1992; **36**:413.
23. Ingber MS, Subia SR, Mondy LA. Massively parallel boundary integral element method modeling of particles in low-Reynolds number Newtonian fluid flows. *Advances in High Performance Computing* 2000; **6**:313–324.
24. Ingber MS, Mondy LA. Direct second-kind boundary integral formulation for Stokes flow problems. *Computational Mechanics* 1993; **11**:11–17.
25. Parsi F, Gadala-Maria F. Fore-and-aft asymmetry in a concentrated suspension of solid spheres. *Journal of Rheology* 1987; **31**(8):725–732.
26. Karnis A, Mason SG. The flow of suspensions through tubes: VI meniscus effects. *Journal of Colloid and Interface Science* 1967; **23**:120–133.
27. Barnes HA. Thixotropy—a review. *Journal of Non-Newtonian Fluid Mechanics* 1997; **70**:1–33.